Imaging of Lipids in Spinal Cord Using Intermediate Pressure Matrix-Assisted Laser Desorption-Linear Ion Trap/Orbitrap MS

ARTICLE *in* ANALYTICAL CHEMISTRY · SEPTEMBER 2009

Impact Factor: 5.64 · DOI: 10.1021/ac901387u · Source: PubMed

5 AUTHORS, INCLUDING:

Rachelle R Landgraf
Wildcat Pharmaceutical Development Center
7 PUBLICATIONS **196** CITATIONS
SEE PROFILE

Maria C Prieto Conaway
Thermo Fisher Scientific
22 PUBLICATIONS **543** CITATIONS
SEE PROFILE

Timothy J Garrett
University of Florida
50 PUBLICATIONS **769** CITATIONS
SEE PROFILE

Richard A Yost
University of Florida
174 PUBLICATIONS **4,478** CITATIONS
SEE PROFILE

Published in final edited form as:
Anal Chem. 2009 October 15; 81(20): 8488–8495. doi:10.1021/ac901387u.

IMAGING OF LIPIDS IN SPINAL CORD USING INTERMEDIATE PRESSURE MALDI-LIT/ORBITRAP MS

Rachelle R. Landgraf[a], **Maria C. Prieto Conaway**[b], **Timothy J. Garrett**[a], **Peter W. Stacpoole**[a], and **Richard A. Yost**[a]

[a] University of Florida, Gainesville, Florida, USA

[b] Thermo Fisher Scientific, San Jose, California, USA

Abstract

A hybrid linear ion trap/Orbitrap mass spectrometer was used to perform MS/MS experiments and high resolution mass analysis of lipids desorbed from nerve tissue. A dramatic improvement in mass spectral resolution and a decrease in background are observed in the spectra collected from the Orbitrap mass analyzer, which allow generation of more accurate mass spectrometric images of the distribution of lipids within nerve tissue. Employment of both mass analyzers provides a rapid and reliable means of compound identification based on MS/MS fragmentation and HRMS accurate mass.

Introduction

The direct interrogation of sectioned tissue by mass spectrometry has piqued the interest of scientists worldwide due to the wide range of molecular species that can be analyzed and the ability to spatially monitor each one. Conventional analyses have been focused on the distribution of proteins and peptides,[1–4] drugs and metabolites,[5–7] and lipids,[8–10] which spans a rather broad mass range. To encompass this range, time-of-flight (TOF) mass spectrometers[11–13] have typically been employed as the mass analyzer of choice. Not only does TOF/MS provide a wide mass range, it offers rapid scan speeds, mass resolution around 10,000, and mass accuracy below 20 ppm.[14]

Improved mass resolution and accuracy have become a center of interest in mass spectrometric imaging as a result of the detection of isobaric species in tissue, particularly in the low mass region. In addition to endogenous compounds, MALDI matrix cluster ions present as isobars adding to the complexity of data analysis because of their potential presence at nearly every m/z value. High-performance instruments, such as Fourier-transform ion cyclotron resonance (FTICR) offer high-resolution scanning (R > 100 000) capable of resolving many ions in a very narrow m/z range (< 1 amu) in a single experiment.[15,16] Along with low-ppm mass accuracy, FTICR demonstrates a methodology highly desirable for the analysis of tissue. However, the technique is hindered by inherently slow scan speeds and often laborious identification of unknowns based solely on accurate mass.

Both TOF/MS and FTICR/MS extend advantages for tissue imaging, but typically offer only one stage of mass analysis. To circumvent this drawback, the addition of an external collision cell[15,16] is often utilized on an FTICR to yield MS/MS data that aid in identification. However, this contributes to extended analysis times. MS/MS spectra are also obtained by isolating the

Correspondence to: Richard A. Yost.

precursor ion in the ICR cell and exciting it with a pulsed laser,[17,18] but fragment energies are often low. TOF/MS renders a more compatible design to the implementation of MS/MS analyses. Post source decay[19,20] is often used due to the ease of execution, but lacks the ability to control fragmentation. TOF/TOF[21,22] and qTOF[23,24] instruments have both been proven to successfully produce MS/MS data, but again, yield relatively low resolution mass spectra and a high degree of fragmentation.

In this study, we describe the use of a hybrid linear ion trap/Orbitrap mass spectrometer with intermediate pressure MALDI for the imaging of lipids in spinal cord. The linear ion trap provides MS^n capabilities, and the Orbitrap analyzer can provide mass resolution of 100,000. This new design affords the ability to identify ions based on MS^n fragmentation and accurate mass and to image the thousands of peaks detected in a single, high-resolution scan as well as high-resolution daughter scans.

Experimental

Animal Treatment and Tissue Preparation

All animal studies were approved by the local IACUC at UCSD and were performed in an AAALAC-approved vivarium. Adult (250–300g body weight) female Sprague-Dawley rats (Harlan, San Diego, CA) were housed 3 per cage under a 12 hr light:dark cycle with free access to food (Harlan Teklad 7001) and water. Excised tissue was immediately flash frozen in liquid nitrogen and stored at −80°C until shipped on dry ice in plastic tubes to the University of Florida, where it was again stored at −80°C until processed. Frozen tissue was sectioned to a thickness of 10 μm at a temperature of −25°C using a Leica CM1850 cryotome (Houston, TX). The tissue was attached to the cryotome sample stage using water to avoid the mass spectral interferences caused by traditional techniques that use polymers to affix the tissue to the sample stage.

Matrix Application

Sectioned tissue was thaw-mounted on glass microscope slides and then dried in a vacuum desiccator for 30 minutes. The matrix, 40 mg/ml 2,5-dihydroxybenzoic acid (DHB) in 70:30 methanol:water with 10 mM sodium acetate, was applied using an Epson R260 inkjet printer.[25] The microscope slides were placed in a modified CD tray holder and passed through the printer 15 times for matrix application. Parameters in the Epson CD printing software were adjusted to give an even coat of matrix across the entire tissue section. Evenness was monitored visually using a dissecting microscope with transmitted illumination through a blue filter.

Instrumentation

Studies were carried out on a hybrid linear ion trap/Orbitrap mass spectrometer fitted with a MALDI ion source that operates at intermediate pressure (MALDI LTQ Orbitrap XL, Thermo Fisher Scientific, Bremen, Germany).26 Briefly, a N_2 laser with a wavelength of 337 nm is focused directly to the source, which operates at a pressure of about ~75 mTorr. The generated MALDI ions are then transferred through a series of differentially pumped quadrupole and octapole ion guides to a linear ion trap where MS^n analysis can be performed or the ions are passed on to the C-trap. These transmitted ions are collisionally cooled in the C-trap before injection into the Orbitrap analyzer for detection or into the high-energy collisional dissociation (HCD) cell for fragmentation. The use of nitrogen at higher pressures in the HCD cell creates higher energy collisions than those typically found in the linear ion trap, which leads to a greater number of fragment ions. The octapole geometry also allows for a lower mass cut off, making detection of low-mass ions possible. Fragment ions produced in the HCD cell are transferred back to the C-trap and injected into the Orbitrap analyzer for detection.

Tissue Analysis

Microscope slides affixed with coated tissue were adhered to a modified MALDI sample plate using copper tape. The laser raster size was set to 100 μm. All experiments were performed with automatic gain control (AGC) turned on, and the signal was optimized by adjusting the laser energy to 15 – 20 μJ. AGC determines (in a prescan event) the number of laser shots to fill either the ion trap or the Orbitrap to a predetermined target value (a dimensionless number that relates to the number of charges allowed into the trap). The default target values were used for all experiments. Both MS and MS^2 experiments were acquired in profile mode. For data acquired on the same section of tissue, the interrogated tissue was first analyzed by the LIT, followed by reinterrogation of the tissue and subsequent analysis performed in the Orbitrap mass analyzer. All other data were acquired on serial sections of tissue. Qualitative data were obtained using standard Xcalibur software and ImageQuest imaging software. Mass spectral images were normalized using the 'MassRange/TIC' plot type in ImageQuest. The intensity axis is normalized to a fixed scale; therefore the colors in the "rainbow" scheme used to display the images correspond to the same intensities. Lipids were identified by correlating the exact masses obtained from high resolution full scan Orbitrap spectra, the characteristic fragmentation patterns from MS^2 spectra, and the distribution of the ions in tissue produced by the mass spectral images. Both the LIT and Orbitrap analyzer were fully tuned and calibrated with the aid of two calibration peptide mixes (MSCal4, Sigma Aldrich, St. Louis, MO, USA) for optimization in two mass ranges: 150–2000 and 200–4000. The mass calibration of the Orbitrap analyzer alone was checked twice a day with external calibrant to ensure operation within the <3 ppm instrument specifications.

Results and Discussion

Orbitrap vs. Linear Ion Trap

Imaging in our lab has typically employed a linear ion trap (LIT) for mass analysis.[27,28] It has proven successful for a wide range of compounds and has been invaluable for identification purposes due to its MS^n capabilities. However, LITs provide only unit resolution and mass accuracy of 100 ppm; often higher resolution and mass accuracy would be helpful in detecting, identifying, and imaging compounds in complex tissue matrices. The Orbitrap mass analyzer offers these advantages with similar limitations in sensitivity to that of the LIT based on the inherent nature of the MALDI technique. The sensitivity in the MALDI technique is best discussed in terms of signal suppression and dynamic range. MALDI in general suffers from ion suppression, especially exacerbated in the case of complex samples such as tissue. The MALDI matrix has been identified as a contributor to ion suppression[29], not only because it is added in excess, but because of its tendency to form adducts, sometimes even interfering with the analytes of interest.[30] The dynamic range in the linear ion trap Orbitrap instrument has been shown to be of the order of 5000:1, intraspectrum, with both electrospray and MALDI sources.[26] The reasons contributing to the high dynamic range are thermalization in the ion source, high capacity of the Orbitrap analyzer, possibility of nitrogen bath gas breaking up the matrix clusters, and possibly, the longer travel time for the ions (compared to TOF).[26]

Figure 1 shows mass spectra of the phospholipid range taken from the same section of rat spinal cord generated from an Orbitrap analyzer (1A) and an LIT (1B). The most notable differences between the spectra are the higher resolving power (R = 100 000 @ m/z 400 for the Orbitrap analyzer vs. R = 4000 for ion traps) and reduction of chemical noise observed in the Orbitrap spectrum. While unit resolution is attained on the LIT, low-abundance ions are masked due to the presence of MALDI matrix ions in the chemical background. Distinguishing ions originating from tissue from those arising from the MALDI matrix is virtually impossible for those that have a signal intensity of less than 10% of the base peak. Examination of the relative abundance of the major ions between the two spectra shows great similarity, but also exhibits

evident differences, notably the increased abundance in the Orbitrap spectrum of nominal m/z values 739, 798, and 866. The accurate masses and fragmentation patterns of these major ions are consistent with two phosphatidylcholine and one cerebroside lipid species: [PC(16:0,18:1) + K − $N(CH_3)_3$]+, $[PC(16:0,18:1) + K]^+$, and $[Cer(d18:1,24:0h) + K]^+$, respectively. Each ion is detected as a potassiated cation. Studies have shown that the alkali metal adducts of lipid ions are more stable in the gas phase than the corresponding protonated species.[31] The lengthened storage time of ions in the Orbitrap analyzer compared to the storage time of a LIT (an order of magnitude difference) may cause loss of the less stable protonated ions while an increased relative abundance is observed for cation species due to greater gas-phase stability.

An advantage of reduced chemical noise for imaging is illustrated in Figure 2. The mass spectrometric images were generated by mapping the total ion current from m/z 450–900 for serial sections of rat spinal cord for data collected on an Orbitrap analyzer (2A) and a LIT (2B). The anatomy of the spinal cord discussed here is illustrated in Figure 2C. A clear tissue shape is observed for both images; the Orbitrap analyzer data, however, shows little or no signal detected off tissue and a distinct gray matter pattern observed as a decrease in signal in the center of the image (seen as a butterfly pattern). The greatest signal detected in the image created by the LIT is in the area off tissue, where only DHB matrix is present. The dominant ion in a DHB spectrum is the M^+ ion at m/z 154. However, DHB readily looses hydrogen and forms adducts with itself and water to form a host of cluster ions that appear at nearly every m/z value in the MALDI spectrum. Following ionization, these matrix cluster ions, along with the analytes of interest, traverse a distance of ~17 cm (two quadrupole ion guides and a set of octapole rods) before reaching the LIT, where they are trapped using helium as a buffer gas. This distance is ~2 times shorter than the distance an ion must travel (~40 cm) through the LIT and another octapole and the C-trap to reach the Orbitrap analyzer. In addition, ions are trapped and collisionally cooled with nitrogen once they are injected into the C-trap. The combination of a longer distance travelled, a longer traverse time, and cooling with a more massive buffer gas in the C-trap may lead to greater dissociation of the matrix cluster ions. Furthermore, the long trapping time required for detection in the Orbitrap analyzer may result in dissociation of loosely bound matrix cluster ions causing further reduction in MALDI matrix background. Preliminary studies in our lab have demonstrated a reduction in DHB matrix background when comparing spectra collected at resolving powers of 7500, 15,000, 30,000, 60,000, and 100,000 (data not shown).

Increasing the acquisition time per scan improves the resolving power (full width at half maximum, FWHM) in the Orbitrap mass spectrometer. For example, a resolution of 60,000 takes 1 sec per scan and a resolution of 100,000 takes 1.9 sec (both defined at m/z 400).[32] The Orbitrap spectrum in Figure 1A took 2.4 sec per pixel to generate with an average of 15 laser shots/pixel. Typical whole spinal cord tissue sections took 30–50 min at a spatial resolution of 100μm (resolving power setting of 60,000). For comparison, preliminary imaging results on an FTICR were reported at 15 sec/pixel.[15] The resolving power in the Orbitrap mass analyzer is inversely proportional to the square root of m/z (for a fixed acquisition time)[32] and therefore diminishes slower than in a FTICR cell (where the resolving power is inversely proportional to m/z). Compared to an FTICR, however, the resolving power of the Orbitrap analyzer is lower (for a given electromagnetic field and up to a certain m/z). For a more detailed discussion on resolving power the interested reader is referred to reference [32]. In the linear ion trap (LIT), in contrast, the peak width (and therefore the resolution) varies only with scan speed. The peak width for ‘normal’ scan rate (16,700 amu/s) is given by the manufacturer as 0.7 amu FWHM. The number of ions in the trap will also affect the isotopic envelope for a peak. The peak width in Fig 1B was measured as ~0.5 amu FWHM for 3 peaks: 782.6, 798.6, and 810.7 for a resolving power m/Δm of 1400–1600. The LIT provides unit resolution throughout the whole mass range up to 4000 at the normal scan rate.

The mass spectral differences between white and gray matter become much more evident with the background reduction observed in the Orbitrap spectra, which could be beneficial to studies tracking changes in specific regions of tissue. Two such ions that exhibit dominance in the differing regions of spinal cord are a phosphatidylcholine at m/z 756 $[PC(16:0,16:0) + Na]^+$ in gray matter and a phosphatidylethanolamine at m/z 776 $[PE(18:0,20:0) + H]^+$ in white matter, which are in agreement with literature values that demonstrate a slightly greater abundance of PCs than PEs in gray matter and a greater abundance of PEs than PCs in white matter.[33] The images of these ions are shown in Figure 3. Figures 3A and 3C are the images of m/z 756 created from data taken on an Orbitrap analyzer and LIT, respectively. When comparing Figures 3A and 3C, increased signal is observed in the white matter region of 3C. A similar effect is perceived in the images of m/z 776. Greater signal is seen in the gray matter section in Figure 3D when compared to Figure 3B. These images provide examples of the increased specificity possible with greatly reduced MALDI matrix background.

Imaging using High Resolution MS Scanning

Mass spectrometric images created from data obtained on mass analyzers that provide unit resolution have provided valuable insight into compound distribution within tissue;[34–36] just as images generated by MS/MS can help differentiate isobaric compounds,[36] so can high resolution MS images, as shown here. Figure 4 shows data obtained on an Orbitrap analyzer. The image seen in Figure 4B was created by mapping a range of m/z values centered at m/z 844.5 amu, plus or minus 0.5 amu. This is the procedure used to produce images from data obtained on a LIT with unit mass resolution. By examining the highly resolved mass spectrum in Figure 4A, one can clearly see that more than one ion is detected at nominal mass 844; mapping a 1 amu range of values produces an image dominated by the base peak of that m/z range, m/z 844.5292 (Figure 4B). Figures 4C – 4E are images crated by mapping the individual ions at m/z 844.4690 ± 0.02, 844.5292 ± 0.02, and 844.9463 ± 0.02, respectively. Two ions, a phosphatidylserine and a phosphatidylcholine, at m/z 844.4690 $[PS(16:0,20:4) + Na + K]^+$ and m/z 844.5292 $[PC(16:0,22:6) + K]^+$ appear in the gray matter of the spinal cord; however, the ion at m/z 844.4690 has a greater distribution throughout all the gray matter, where the ion at m/z 844.5292 appears to be less abundant in the dorsal horns. The image of m/z 844.9463 (unidentified) is opposite of the other two ions and appears only in white matter. This ion is completely masked when imaging a range of values (4B), which illustrates the importance of high resolution analysis of complex samples such as tissue.

The Role of HRMS and MS/HRMS in Identifying Lipids

The identification of ions based solely on accurate mass is a tedious process due to the immense number of elemental compositions comprising the ions detected in nerve tissue. First, mass accuracy must be considered to give an accurate representation of the elemental composition. For example, two dominant peaks are detected at nominal mass 832 which are 832.5865 and 832.6671 and are consistent with $[PC(18:0,20:4) + Na]^+$ and $[Cer(d18:1,24:1) + Na]^+$, respectively. Accurate mass calculations of the two ions produce a mass of 832.5832 (2.9 ppm error) for the PC and 832.6642 (3.3 ppm error) for the Cer. The difference in masses for the observed values is 0.0806, and the difference in the calculated values is 0.0810 (0.4 ppm error).

If determining the elemental composition (PC: $C_{46}H_{84}NO_8P$; Cer: $C_{48}H_{91}NO_8$) of these two ions is attempted based solely on the molecular weight and with no limitations, a list is generated that contains hundreds of possible combinations. By applying a constraint to include only those combinations within the mass error, 3 possible elemental compositions are given for the Cer and 13 are given for the PC. Of these likely combinations, only 2 from each list are reasonable for lipid ions. However, there is no distinction between isomeric compounds. A Cer would not have any isomers because of the lack of a phosphorus atom, but a PE ion with a fatty acid composition of (41:4) has the same molecular formula as a PC with a fatty acid

composition of (38:4). While odd chained fatty acids are not common, the possibility of a lipid containing such a fatty acid can not be ignored nor confirmed without the use of MS/MS.

MS/MS has proved to be invaluable for the identification and differentiation of isobaric/isomeric species. Product ions in the MS/MS spectrum have allowed identification of lipid classes based on characteristic fragmentation (i.e. neutral losses of 43, 59, and 87 for PEs, PCs, and PSs, respectively) as well as fatty acid tail assignment based on relative intensity of the fragment. Images generated from these characteristic fragments show distinct differences in distribution within the tissue.[35]

The roles of high mass accuracy and MS/MS have both been employed here to provide highly dependable identification of lipid ions. An expansion of the m/z range 848 – 849 on the Orbitrap spectrum in Figure 1A can be seen in Figure 5A. At least four ions are detected within this mass range; the images corresponding to m/z 848.5603, 848.6417, and 848.6617 are shown in 5B – 5D. The ion at m/z 848.6975 is too low in abundance to produce a useful image. The distribution of ions in Figures 5C and 5D are very similar within the white matter, whereas the ion in Figure 5B is distributed only in the gray matter.

Isolation of the ions at m/z 848.5 ± 0.5 in the linear ion trap and subsequent fragmentation in the LIT produces the Orbitrap analyzer MS/MS spectrum given in Figure 5E. The product ion at m/z 830.6493 arises from a neutral loss (NL) of 18 (water) and is a common fragment among biomolecules. The product ion at m/z 789.4846 is a NL of 59 and arises from the loss of the choline head group, $N(CH_3)_3$, from a PC. A low abundance product ion at m/z 761.4536 arises from a NL of 87 and is consistent with the loss of the serine head group ($C_3H_5NO_2$) of a PS ion. The product ions at m/z 686.6062, 668.5962, 512.5208, and 484.3260 all correspond to losses associated with a Cer ion. The NL of 162 (m/z 686.6062) is a loss of $C_6H_{10}O_5$ from the head group, the NL of 180 (m/z 668.5962) is a loss of the galactose head group, m/z 512.5208 is the loss of the fatty acid tail after the carbonyl, and m/z 484.3260 is the loss of the entire fatty acid tail. The image created using product ion of m/z 848 at 789.4846 (Figure 5F) matches the pattern of the image of the full scan m/z 848.5603 (Figure 5B), which indicates that the latter m/z value corresponds to a PC. Performing an exact mass calculation (848.5572) makes this ion consistent with $[PC(18:0,20:4) + K]^+$. The images produced from the four Cer product ions all exhibit the same pattern, so only the image created by m/z 484.3260 (Figure 5G) was chosen for comparison. The pattern matches that of the images for the m/z values 848.6417 and 848.6617 (Figures 5C and 5D, respectively) in the full-scan mass spectrum. This suggests that both these isobaric ions could be Cers. The product ion arising from the NL of 87 is too low in abundance to give a useful image; however, the calculated exact mass for a PS (most likely $[PS(18:1,18:1) + Na + K]^+$) would be detected at 848.4812, which eliminates the possibility of the ion at m/z 848.6417 being a PS.

Several possibilities exist for the identification of Cers due to the possible hydroxylation of the C2 carbon in the fatty acid. The NL of ~364 between the parent ions at mass 848.6417 or 848.6617 and 484.6975 suggests a fatty acid with either 24 or 25 carbons. By calculating exact masses, three Cers are consistent with nominal mass 848: $[Cer(d18:1,24:1) + K]^+$ 848.6382; $[Cer(d18:1,24:1h) + Na]^+$ 848.6592; $[Cer(d18:1,25:0) + Na]^+$ 848.6955. The exact masses for these three ions have mass discrepancies of 0.0035, 0.0025, and 0.0020, respectively, from the masses detected in the full-scan mass spectrum (848.6417, 848.6617, and 848.6975). The mass discrepancy for $[PC(18:0,20:4) + K]^+$ detected at m/z 848.5603 is 0.0031. The mass error for all the ions is within the range of that discussed previously in this section. Therefore, a high degree of confidence in correct identification is maintained. The structures for each lipid ion discussed here are proposed in Figure 6 along with corresponding NLs and characteristic fragments.

Conclusions

The utility of imaging mass spectrometry using a hybrid LIT/Orbitrap mass spectrometer for analysis of lipids in spinal cord is clearly demonstrated, and results showed that each mass analyzer on its own provides a unique way of analyzing the wealth of information obtained. While each mass analyzer can stand alone for imaging MS, with MS/MS provided by the LIT and HRMS by the Orbitrap analyzer, combining the two, provides a superior method for the analysis of complex tissue.

Acknowledgments

We thank Dr. Nigel Calcutt at the University of California at San Diego for providing the spinal cord tissue. We acknowledge the NIH (RO1 ES007355) and NSF PIRE program (OISE-0730072) for support of this project

Reference List

1. Seeley EH, Caprioli RM. Proceedings of the National Academy of Sciences of the United States of America 2008;105:18126–18131. [PubMed: 18776051]
2. Ceuppens R, Dumont D, Van Brussel L, Van de Plas B, Daniels R, Noben JP, Verhaert P, Van der Gucht E, Robben J, Clerens S, Archens L. Journal of Mass Spectrometry 2007;260:185–94.
3. DeKeyser SS, Kutz-Naber KK, Schmidt JJ, Barrett-Wilt GA, Li L. Journal of Proteome Research 2007;6:1782–91. [PubMed: 17381149]
4. Verhaert PD, Prieto Conaway MC, Pekar TM, Miller K. International Journal of Mass Spectrometry 2007;260:177–84.
5. Wiseman JM, Ifa DR, Zhu Y, Kissinger CB, Manicke NE, Kissinger PT, Cooks RG. Proceedings of the National Academy of Sciences of the United States of America 2008;105:18120–18125. [PubMed: 18697929]
6. Drexler DM, Garrett TJ, Cantone JL, Diters RW, Mitroka JG, Prieto Conoway MC, Adams SP, Yost RA, Sanders M. Journal of Pharmacological and Toxicological Methods 2007;55:279–88. [PubMed: 17222568]
7. Stoeckli M, Staab D, Schweitzer A. International Journal of Mass Spectrometry 2007;260:195–202.
8. Shimma S, Sugiura Y, Hayasaka T, Hoshikawa Y, Noda T, Setou M. Journal of Chromatography B 2007;855:98–103.
9. Amaya KR, Monroe EB, Sweedler JV, Clayton DF. International Journal of Mass Spectrometry 2007;260:121–27.
10. Borner K, Malmberg P, Mansson JE, Nygren H. International Journal of Mass Spectrometry 2007;260:128–36.
11. Li Y, Shrestha B, Vertes A. Analytical Chemistry 2008;80:407–20. [PubMed: 18088102]
12. Hsieh Y, Chen J, Korfmacher W. Journal of Pharmacological and Toxicological Methods 2007;55:193–200. [PubMed: 16919485]
13. Groseclose MR, Andersson M, Hardesty WM, Caprioli RM. Journal of Mass Spectrometry 2007;47:254–62. [PubMed: 17230433]
14. Mirsaleh-Kohan N, Robertson WD, Compton RN. Mass Spectrometry Reviews 2008;27:237–85. [PubMed: 18320595]
15. Cornett DS, Frappier SL, Caprioli RM. Analytical Chemistry 2008;80:5648–53. [PubMed: 18564854]
16. Taban IM, Altelaar AFM, van der Burgt YEM, McDonnell LA, Heeren RMA. Journal of the American Society for Mass Spectrometry 2007;18:145–51. [PubMed: 17055739]
17. Dodds ED, German JB, Lebrilla CB. Analytical Chemistry 2007;79:9547–56. [PubMed: 18001128]
18. Dodds ED, Hugerman PJ, Lebrilla CB. Analytical Chemistry 2006;78:8506–11. [PubMed: 17165846]
19. Kenny DJ, Brown JM, Palmer ME, Snel MF, Bateman RH. Journal of the American Society for Mass Spectrometry 2006;17:60–66. [PubMed: 16352437]
20. Clipston NL, Jai-nhuknan J, Cassady CJ. International Journal of Mass Spectrometry 2003;222:363–81.

21. Vaezzdeh AR, Simicevic J, Chauvet A, Francois P, Zimmermann-Ivol CG, Lescuyer P, Deshusses JPM, Hochstrasser DF. Rapid Communications in Mass Spectrometry 2008;22:2667–76. [PubMed: 18677718]
22. Lemaire R, Desmons A, Tabet JC, Day R, Salzet M, Fournier I. Journal of Proteome Research 2007;6:1295–305. [PubMed: 17291023]
23. Signor L, Varesio E, Staack R, Starke V, Richter WF, Hopfgartner G. Journal of Mass Spectrometry 2007;42:900–09. [PubMed: 17534860]
24. Hsieh Y, Casale R, Fukuda E, Chen J, Knemeyer I, Wingate J, Morrison R, Korfmacher W. Rapid Communications in Mass Spectrometry 2006;20:965–72. [PubMed: 16470674]
25. Baluya DL, Garrett TJ, Yost RA. Analytical Chemistry 2007;79:6862–67. [PubMed: 17658766]
26. Strupat, Kerstin; Kovtoun, V.; Bui, H.; Viner, Rosa; Stafford, G.; Horning, S. Journal of the American Society for Mass Spectrometry 2009;20:1451–63.
27. Garrett, TJ.; Yost, RA. Mass Spectrometric Imaging. Rubakhin, SS.; Sweedler, JV., editors. Humana Press; New York: 2009.
28. Garrett, TJ.; Yost, RA. Practical Aspects of Trapped Ion Mass Spectrometry. March, RE.; Todd, JFJ., editors. Vol. Chapter 10. CRC Press; Boca Raton: 2008.
29. Knochenmuss R, Zenobi R. Chemical Reviews 2003;103:441–52. [PubMed: 12580638]
30. Krutchinsky A, Chait BT. Journal of the American Society for Mass Spectrometry 2002;13:129–34. [PubMed: 11838016]
31. Garrett, TJ. PhD Dissertation. University of Florida; 2006.
32. Makarov A, Denisov Eduard, Kholomeev Alexander, Balschun Wilko, Lange Olvier, Strupat Kerstin, Horning Stevan. Analytical Chemistry 2006;78:2113–20. [PubMed: 16579588]
33. Agranoff, BW.; Benjamins, JA.; Hajra, AA. Basic Neurochemistry: Molecular, Cellular and Medical Aspects. Vol. 6. Siegel, GJ.; Agranoff, BW.; Fisher, SK.; Lbers, RW.; Uhler, MD., editors. Vol. Chapter 3. Lippincott-Raven; Philadelphia: 1998.
34. Prieto Conaway MC, Bui H, Beachy S, Pitoniak R, Hylander B, Wang P, Marlar K, Repasky E, Kazim L. LC-GC Europe 2008, Applications Book :14.
35. Garrett TJ, Prieto-Conaway MC, Kovtoun V, Bui H, Iagarian N, Stafford G, Yost RA. International Journal of Mass Spectrometry 2007;260:166–76.
36. Cha S, Yeung ES. Analytical Chemistry 2007;79:2373–85. [PubMed: 17288467]

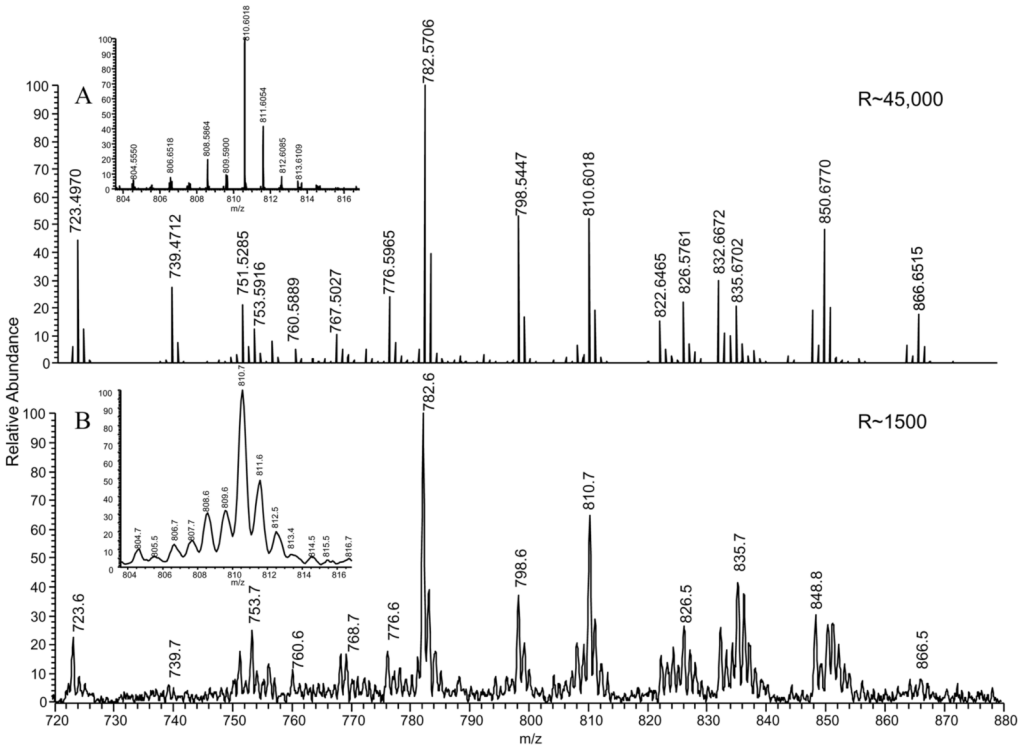

Figure 1.

Mass spectra of the phosphlipid m/z range of a section of rat spinal cord. Each spectrum represents the same area of spinal cord tissue analyzed by (A) an Orbitrap analyzer and (B) a linear ion trap. The insets show a 12 amu mass range centered around m/z 810.

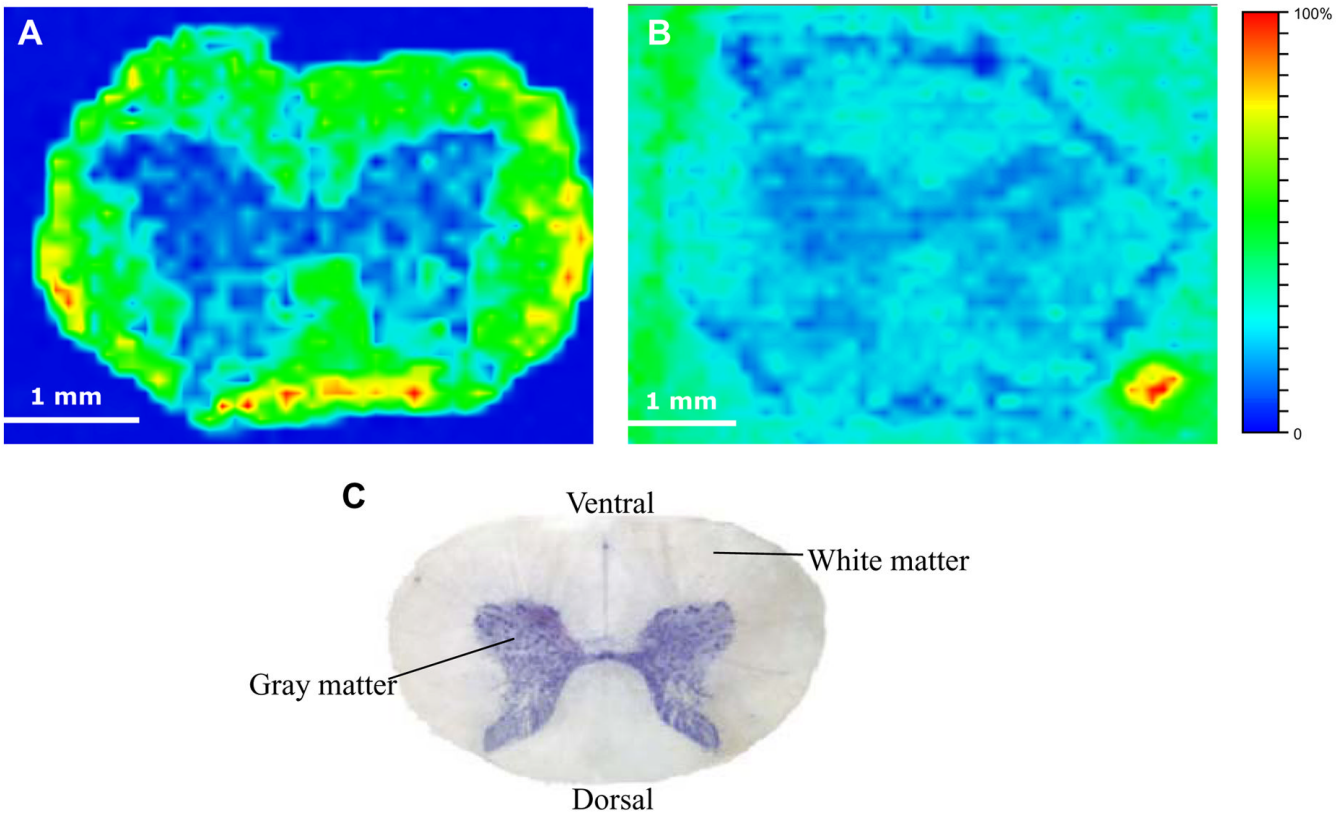

Figure 2.

Mass spectrometric images of the total ion current of serial rat spinal cord sections analyzed by (A) an Orbitrap analyzer and (B) a linear ion trap. Basic anatomical structure is labeled in C (from Freir, MA; Tourinho, SC; Guimaraes, JS; Oliveira, JLF; Picanco-Diniz, CW; Gomes-Leal, W; Pereira, A Jr. *Frontiers in Neurochemistry*, **2008**, *2*, 1–9).

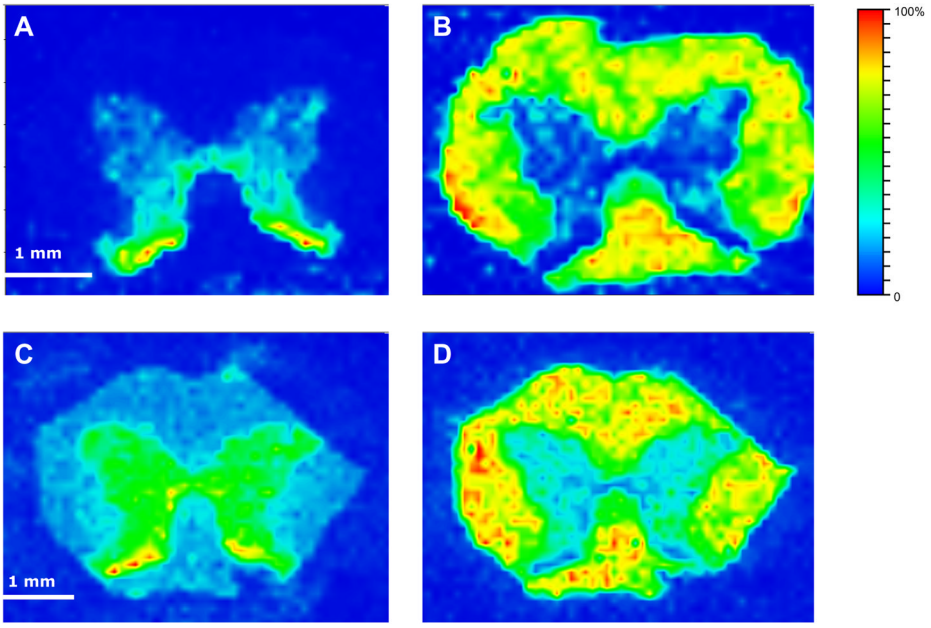

Figure 3.

Mass spectrometric images of m/z 756 (A,C) and m/z 776 (B,D) generated from serial rat spinal cord sections analyzed on (A,B) an Orbitrap analyzer and (C,D) a linear ion trap. The ion at m/z 756 is dominant in the gray matter of the spinal cord where the ion at m/z 776 is dominant in the white matter.

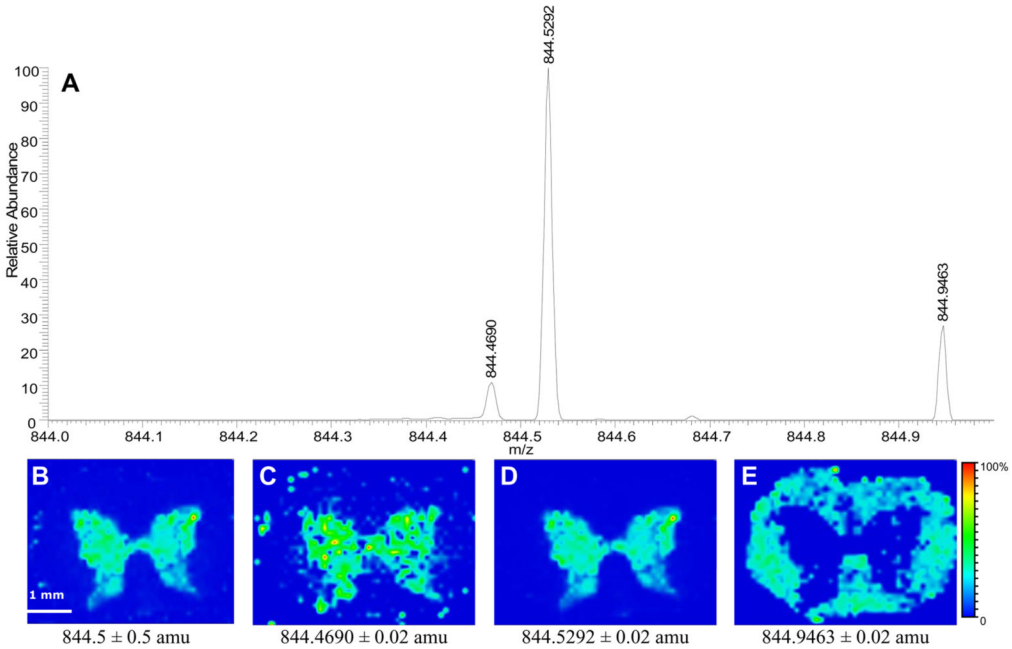

Figure 4.

(A) Mass spectrum of m/z region 844–845 showing at least 5 peaks are detected. The mass spectrometric images correspond to (B) the 1 amu mass range and the peaks at (C) 844.4690, (D) 844.5292, and (E) 844.9463.

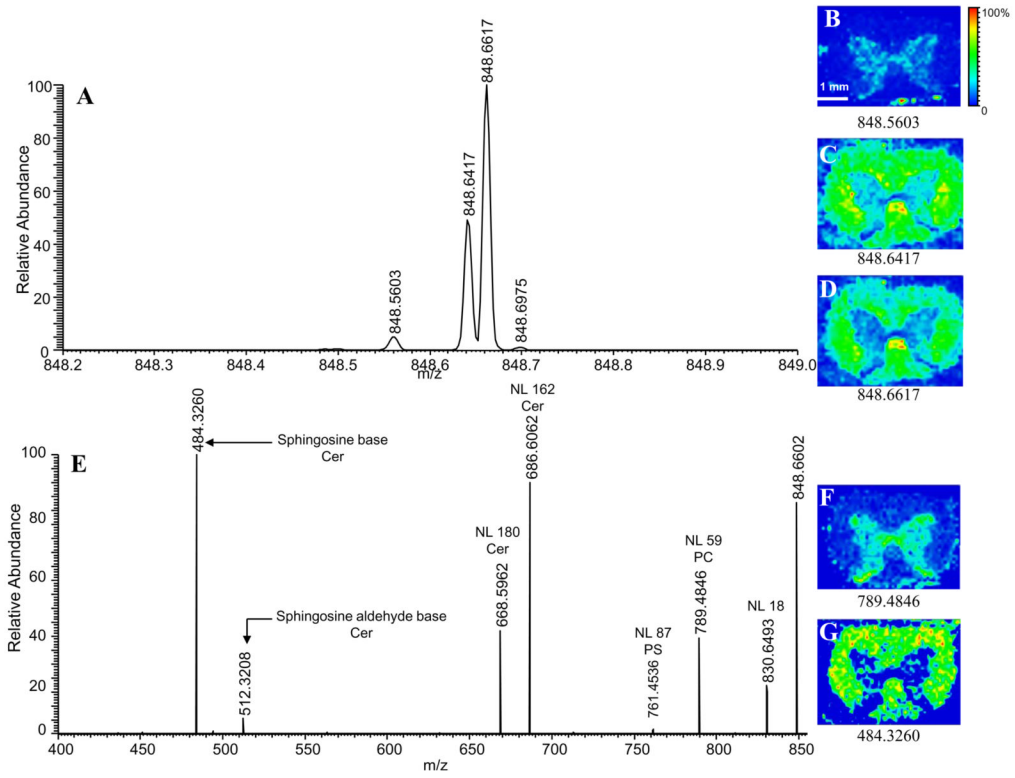

Figure 5.

(A) Mass spectrum of m/z region 848–849 acquired on an Orbitrap analyzer. Mass spectrometric images B–D correspond to major ions detected in A. Fragmentation of nominal m/z 848 in the linear ion trap produces the MS/MS spectrum seen in E. Images observed in F and G corresponds to the two major isobars found at 848. Matching images produced by the full scan and MS/MS spectra and exact mass calculations identify the ions in the full scan mass spectrum as: 848.5603 [PC(18:0,20:4) + K]+; 848.6417 [Cer(d18:1,24:1) + K]+; 848.6617 [Cer(d18:1,24:1h) + Na]+; 848.6975 [Cer(d18:1,25:0) + Na]+. NL: neutral loss; PC: phosphatidylcholine; PS: phosphatidylserine; Cer: cerebroside

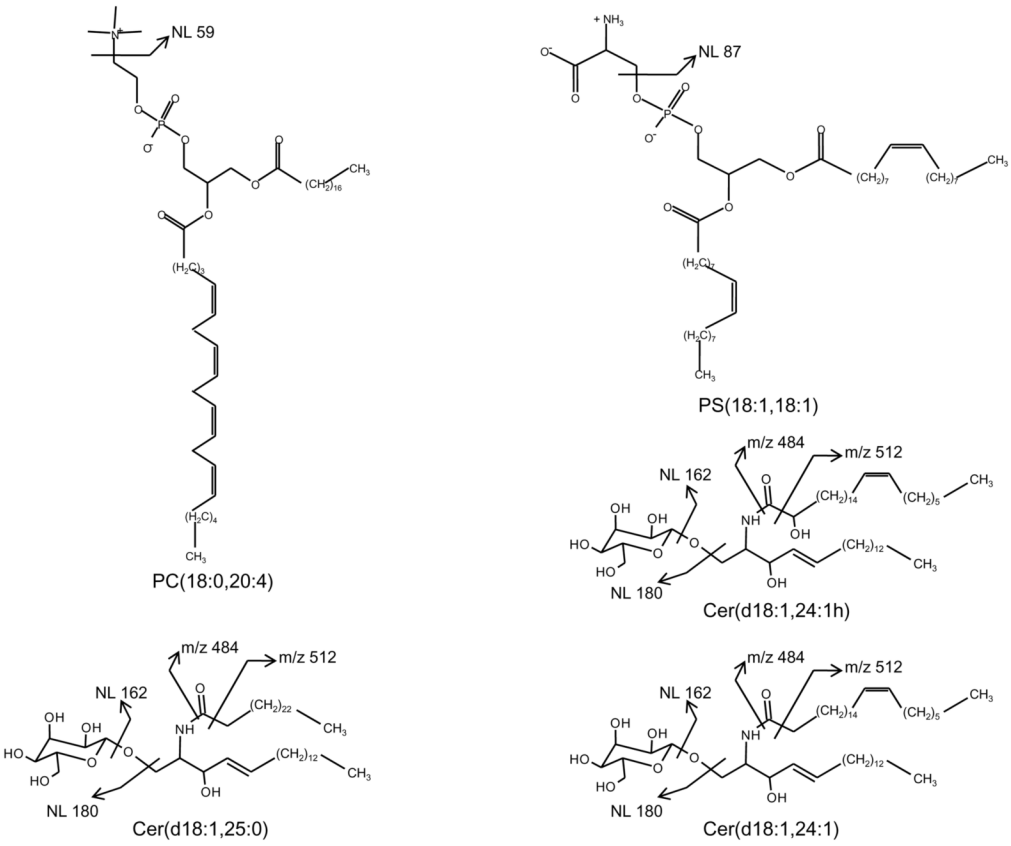

Figure 6.
Proposed lipid structures and corresponding neutral losses and characteristic fragments for nominal m/z 848.